Towards Understanding the History and Mechanisms of Martian Faulting. L. L. Dimitrova[1], W. E. Holt[1], A. J. Haines[2] and R. A. Schultz[3], [1]Department of Geosciences, SUNY at Stony Brook, Stony Brook, NY 11794 (Lada.Dimitrova@stonybrook.edu, William.Holt@stonybrook.edu), [2]Department of Earth Sciences, University of Cambridge, UK (ajh50@cam.ac.uk), [3]Department of Geological Sciences and Engineering, University of Nevada, Reno, NV (schultz@mines.unr.edu).

Introduction: An understanding of the sources of stress, and the expected style, orientation, and magnitudes of stress and associated strain is important for understanding the evolution of faulting on Mars and its relationship to loading, thus leading to an improved understanding of Martian geologic history and surface morphology. The Tharsis province, characterized by radial graben sets and circumferential wrinkle ridges [1, 2, 3], has been intensely studied since the Viking missions. More recently, the analysis was extended using MGS topography and gravity data [4], and [5] furthermore argued that the faulting is explained by membrane flexure alone.

[4] calculated the deflection of the lithosphere due to the Tharsis load alone while satisfying the long wavelength signal of present day topography and gravity. The resulting extensional component of the stresses and strains is consistent with normal faulting on pre-existing faults radial to Tharsis and away from the load, e.g. Memnonia, Thaumasia, southern Claritas, and Tempe Fossae. However, the faulting extending from northern Claritas Fossae north to Tantalus and Alba Fossae is not well explained by the membrane model, which predicts zero extension there, where the density of normal faults is high [1].

Therefore, these faults may have formed under different conditions (topography and gravity) than we see today [4]. In particular, while the bulk of the crust formed 4.5 Ga and later additions were volumetrically minor [6], gravity and elastic thicknesses are unlikely to have remained unchanged for the last 4.5 Gy. It is conceivable that mantle circulation rather than flexure played a significant role in the early support of Tharsis, producing a different gravity field during that time [7].

We consider a different source of stress – stress associated with internal buoyancy forces, i.e., gravitational potential energy (GPE), constrained by MGS topography and crustal thickness models of [8]. To test the validity of these stress models, we compare results with the style and orientation of the surface faults.

Lithospheric Stress Models: We solve the force-balance equations for the vertically integrated deviatoric stress field associated with topography and crustal thickness variations as the unique solution that balances the body force distribution, in this case GPE differences, while providing a global minimum of the second invariant of stress [9]. The solution is computed over a global grid of 0.25 × 0.25 resolution, assuming ρ_{crust} = 2900 kg.m^{-3}, ρ_{mantle} = 3500 kg.m^{-3}, g = 3.7 m.s^{-2}, various lithospheric depths and rheologies.

Results: The Martian deviatoric stress field associated with horizontal GPE gradients for an incompressible elastic rheology shows, to first order, deviatoric extension over topographically high areas transitioning to deviatoric compression at topographically low areas (Fig. 1) [see also 10]. A notable exception to this pattern is areas with low topography but thin crust, which exhibit propensity for deviatoric extension, e.g., Isidis Planitia and to a smaller extent Utopia, Argyre, and Acidalia Planitae.

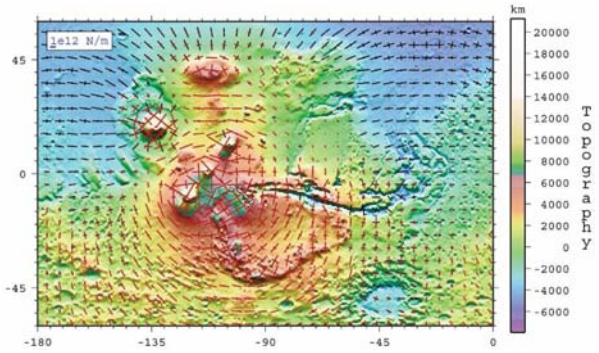

Figure 1. Global variation of vertically integrated deviatoric lithospheric stresses associated with GPE variations. Red and black arrows represent deviatoric extension and compression respectively.

A normalized fault style parameter based on relations among the styles of faulting in the upper crust and the deviatoric principal stresses [11] is shown in Fig. 2. Apart from the exceptions already noted in connection with low topography and thin crust, normal faulting is predicted as the dominant fault style for topographically high areas, thrust faulting for topographically low areas, and strike-slip faulting potentially in between.

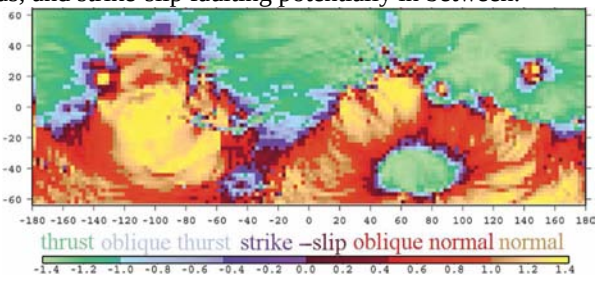

Figure 2. Predicted fault style for GPE stresses.

For each area with fault data, we perform a Kostrov moment tensor summation to estimate the total strain

tensor [12] and define objective function M_{full} that measures the misfit between the dynamically predicted stress field and the strain from fault observations [13]. M_{full} is minimized when the tensor solution of stress or strain from the dynamic calculations is consistent with the formation of faults with the same strike and style as the fault data; thus, it accounts for fault strike and fault style, defined by the relative magnitudes of the principal axis of the stress tensor. M_{full} has values from 0 to 1, with 0 misfit indicating a perfect fit.

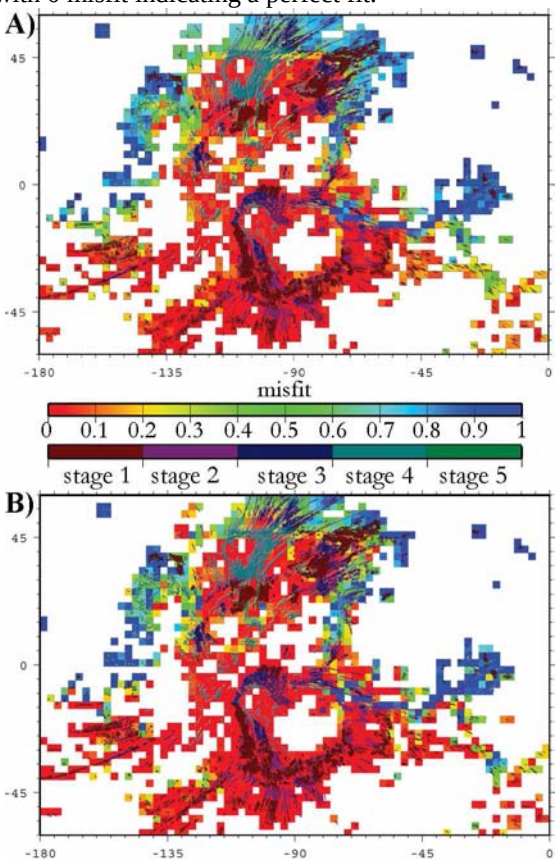

Figure 3. The misfit A) M_{full} and B) $M_{pre\text{-}existing}$ between the normal faults identified by [1] and the GPE stress model overlain by the normal faults (stage 1:Noachian, stage 2: Late Noachian-Early Hesperian, stage 3: Early Hesperian, stage 4: Late Hesperian-Early Amazonian, stage 5: Middle-Late Amazonian).

Fig 3A shows the misfit M_{full} of 19,897 normal fault segments as identified in [1] with our GPE model from Fig. 1. We have assumed a uniform amount of slip for each fault as a first approximation since the misfit function M_{full} is insensitive to scalar multiples of the slip for each fault. The GPE model fits a large fraction of the faults (69% of fault length has $M_{full} \leq 0.1$).

Since M_{full} reflects misfit to both fault strike and style, we define a misfit function $M_{pre\text{-}existing}$ [13], which measures if the model stress field is aligned with the prescribed fault strike such as to produce the style of faulting, in our case normal faulting, and ignores any along strike stresses. $M_{pre\text{-}existing}$ is plotted in Fig. 3B, and overall only a slight improvement to the fit is observed (71% of fault length has $M_{pre\text{-}existing} \leq 0.1$).

A few areas show a marked improvement (much lower $M_{pre\text{-}existing}$ than M_{full}), e.g., the east-west fault at 170-157.5°W;-15°S, indicating that there we largely misfit the relative magnitudes of the along-strike stress as compared to the fault-normal stress. Otherwise, in areas of misfit to the normal faults, the misfit is to both the stress orientation and the fault-normal stress style.

A preliminary investigation of the shortening directions of wrinkle ridges shows that while the fit to the wrinkle ridges in Solis and southern Lunae Planae is poor, our GPE deviatoric stresses fit a large portion of the wrinkle ridges in the northern plains [14].

It is possible that that the misfit to some of the isolated small segments, e.g., Olympus Mons and Margaritifer Terra, can be explained by misregistration of the pre-MGS dataset of [1] to the MOLA data; however, small rotations and translations of the large scale groups of segments along the northern portions of Alba, Tantalus, Mareotis, and Tempe Fossae will not improve the fit significantly there. Finally, we calculate vertically integrated deviatoric stresses, and thus it is possible that the misfitted faults were created in response of near-surface stress that is not representative of the entire column, as may happen for example for shallow faults in the presence of a detachment layer.

Discussion: A deviatoric stress field associated with horizontal gradients of GPE provides an excellent fit to most of the normal faults in Tharsis as well as many wrinkle ridges circumferential to Tharsis. This suggests that many of the faults were created at times when elastic thicknesses and membrane and flexural stresses were small, a combination of brittle and ductile deformation was likely to be widespread, and GPE stresses dominated. Virtually all the misfit associated with GPE alone can be removed by adding membrane stresses associated with very modest deflections of the lithosphere (92% of fault length has $M_{full} \leq 0.1$).

References: [1] Anderson et al. (2001) *JGR, 106,* 20563. [2] Withers P. and Neumann G. (2001) *Nature, 410,* 651. [3] Head et al. (2002) *doi:10.1029/2000JE001445*. [4] Banerdt W. B. and Golombek M. (2000) *LPS XXXI,* Abstract #2038. [5] Phillips et al. (2001) *Science, 291,* 2587. [6] Nimmo F. and Tanaka K. (2005) *Annu. Rev. EPS, 33,* 133. [7] Lowry A.R. and Zhong S.J. (2003) *JGR, 108,* 5099. [8] Neumann G.A. et al. (2004) *doi:10.1029/2004JE002262*. [9] Flesch L. et al. (2001) *JGR, 106,* 16435. [10] Dimitrova L.L. et al (2005) *LPS XXXVI,* Abstract #2039, 2051. [11] Anderson, E.M. (1951) *The Dynamics of faulting and dike formation*. [12] Schultz R.A. (2003) *doi:10.1029/2002GL016475*. [13] Dimitrova L.L. et al (2006) *GRL, in review*. [14] Montési L.G.J. and Zuber M.T. (2003) doi:10.1029/2002JE001974.